

Research paper

Heat transfer coefficients and productivity of a single slope single basin solar still in Indian climatic condition: Experimental and theoretical comparison



Abhay Agrawal^{a,*}, R.S. Rana^b, Pankaj K. Srivastava^a

^a Department of Mechanical Engineering, Rewa Engineering College, P-2, Engineering College Colony, University Road, Rewa 486002, MP, India

^b Department of Mechanical Engineering, Maulana Azad National Institute of Technology, Bhopal, MP, India

ARTICLE INFO

Article history:

Received 3 February 2017

Revised 12 April 2017

Accepted 17 May 2017

Available online 5 June 2017

Keywords:

Single sloped solar still

Basin liner

Nocturnal output

Attenuation factor

Distillate output

ABSTRACT

A theoretical and experimental study was conducted at the central Indian location of Rewa, M.P., India (Latitude: 24°33' 20.81" N, Longitude: 81°18' 49.1" E). This paper presents a detailed comparison of the theoretical and the experimental results obtained for a single sloped basin type solar still. Results for different parameters such as basin water temperature, glass cover temperature, distillate output, evaporative, convective and radiative heat transfer coefficients and attenuation factor were obtained for basin water depths ranging from 2 cm to 10 cm. For solar still, daily distillate output decreased with increase in basin water depth. The theoretical value of daily efficiency for 2 cm and 10 cm basin water depth was around 52.83% and 41.75%, respectively, and for the same basin water depth, experimental daily efficiency was around 41.49% and 32.42% respectively. A sound agreement between the theoretical and the experimental results was observed.

© 2017 Tomsk Polytechnic University. Published by Elsevier B.V.
This is an open access article under the CC BY-NC-ND license.
(<http://creativecommons.org/licenses/by-nc-nd/4.0/>)

1. Introduction

Nectar is found on earth in the form of water. There is an urgent need of fresh water for the survival of human beings, as without water life is not possible on our planet. More than two third of the earth's surface is covered with water. Ninety-seven percentage of water resources on the earth's surface are found in the form of oceans and seas which contain highly salty water (3000 ppm to 35,000 ppm) and therefore not suitable for human consumption. Only 3% of total water resources on the earth's surface have clean water. More than 2% of fresh water is frozen in the form of glaciers and ice blocks in the polar region and rest of fresh water (less than 1%) is found in the rivers, ponds, lakes and underground water. That small part of fresh water has been the main source of water to fulfill the demand for domestic, agricultural, and industrial activities.

Actually, this fresh water is not fresh according to the international standard as it contains the harmful bacteria and viruses, which are the cause of various water-generated diseases such as cholera, diarrhea, malaria, typhoid and many more, which kill over

3 million people every year. Clean water is a precious commodity and very important for our survival. Due to increase in population and fast industrial development, the requirement of potable water will increase day by day. More and more water purification systems are being developed to cope with fresh water scarcity on the earth. One of the process known as distillation can fulfill this. It is a widely accepted process for converting brackish or impure water into drinkable water by the application of thermal energy (solar or fossil fuels). Solar energy is an ideal solution for powering the distillation process, which is environment friendly, free of cost, never lasting and abundantly available all over the planet.

Solar distillation is one of the best methods for purifying brackish water. Solar still is a device which is widely used in the solar distillation process, but the efficiency and productivity of a solar still is very low as compared to other distillation processes, hence it is necessary to enhance the productivity of solar still by improving the conventional design parameters and operational procedures.

The construction of a solar still is very simple. Local people using locally available material can make it. Still is an airtight black painted rectangular basin enclosed by transparent cover to trap the solar energy inside it and contains impure water. When sun light falls on transparent cover, basin water is heated and gets evaporated. The water vapor condenses on the inner side of the

* Corresponding author.

E-mail address: abhayagrwalgec@gmail.com (A. Agrawal).

Nomenclatures

A_b	Basin liner surface area of still (m^2)
A_s	Basin side wall area of still (m^2)
C_w	Specific heat of water in solar still ($J/kg\ ^\circ C$)
C_i	Specific heat of insulation in still ($J/kg\ ^\circ C$)
d_w	Water depth in basin (m)
h_{cwg}	Convective heat transfer coefficient from basin water to glass cover ($W/m^2\ ^\circ C$)
h_{ewg}	Evaporative heat transfer coefficient from basin water to glass cover ($W/m^2\ ^\circ C$)
h_{rwg}	Radiative heat transfer coefficient from basin water to glass cover ($W/m^2\ ^\circ C$)
h_{twg}	Total heat transfer coefficient from basin water to glass cover ($W/m^2\ ^\circ C$)
h_{cga}	Convective heat transfer coefficient from glass cover to ambient ($W/m^2\ ^\circ C$)
h_{rga}	Radiative heat transfer coefficient from glass cover to ambient ($W/m^2\ ^\circ C$)
h_{tga}	Total heat transfer coefficient from glass cover to ambient ($W/m^2\ ^\circ C$)
h_{cbw}	Convective heat transfer coefficient from basin liner to water ($W/m^2\ ^\circ C$)
h_{tba}	Total heat transfer coefficient from basin liner to ambient ($W/m^2\ ^\circ C$)
h_{ba}	Total heat transfer coefficient from bottom of basin to ambient ($W/m^2\ ^\circ C$)
h_{cba}	Convective heat transfer coefficient from bottom of basin to ambient ($W/m^2\ ^\circ C$)
h_{rba}	Radiative heat transfer coefficient from bottom of basin to ambient ($W/m^2\ ^\circ C$)
$I(t)$	Solar Intensity (W/m^2)
K_i	Thermal conductivity of insulation ($W/m\ ^\circ C$)
L_{ev}	Latent heat of vaporization of water (J/kg)
L_i	Thickness of insulation (m)
m_w	Mass of water in basin (Kg)
M_w	Hourly distillate output per unit basin area ($Kg/m^2/h$)
M'_w	Daily distillate output per unit basin area ($Kg/m^2/d$)
p_w	Partial saturated vapor pressure at a basin water temperature (N/m^2)
P_g	Partial saturated vapor pressures at glass cover temperature (N/m^2)
q_{cwg}	Convective heat transfer from basin water to glass cover (W/m^2)
q_{ewg}	Evaporative heat transfer from basin water to glass cover (W/m^2)
q_{rwg}	Radiative heat transfer from basin water to glass cover (W/m^2)
q_{twg}	Total heat transfer from basin water to glass cover (W/m^2)
q_{cga}	Convective heat transfer from glass cover to ambient (W/m^2)
q_{rga}	Radiative heat transfer from glass cover to ambient (W/m^2)
q_{tga}	Total heat transfer from glass cover to ambient (W/m^2)
q_{cbw}	Convective heat transfer from basin liner to water (W/m^2)
q_{tba}	Total heat transfer from basin liner to ambient (W/m^2)
q_{ba}	Total heat transfer from bottom of basin to ambient (W/m^2)

q_{cba}	Convective heat transfer from bottom of basin to ambient (W/m^2)
q_{rba}	Radiative heat transfer from bottom of basin to ambient (W/m^2)
R_g	Reflectivity of glass cover
R_w	Reflectivity of basin water
R_g	Reflectivity of basin liner
t	Time interval (s)
t_g	Glass cover thickness (m)
T_g	Glass cover temperature ($^\circ C$)
T_w	Basin water temperature ($^\circ C$)
T_b	Basin liner temperature ($^\circ C$)
T_a	Ambient temperature ($^\circ C$)
T_{sky}	Sky temperature ($^\circ C$)
U_b	Overall bottom heat transfer coefficient from bottom to ambient ($W/m^2\ ^\circ C$)
U_t	Overall top heat transfer coefficient from basin water to ambient ($W/m^2\ ^\circ C$)
U_L	Overall heat transfer coefficient for still ($W/m^2\ ^\circ C$)
V_w	Velocity of Wind (m/s)

Greek symbols

α_g	Absorptivity of glass cover
α_w	Absorptivity of basin water
α_b	Absorptivity of basin liner
α'_g	Fraction of solar flux absorbed by a glass cover
α'_w	Fraction of solar flux absorbed by basin water
α'_b	Fraction of solar flux absorbed by basin liner
ε_g	Emissivity of glass cover
ε_w	Emissivity of basin water
ε_b	Emissivity of basin liner
ε_{eff}	Effective emissivity between water surface and glass cover
σ	Stefan–Boltzmann constant
μ_j	Fraction of solar flux having extinction coefficient
η_j	Extinction coefficient
η	Efficiency of solar still

Subscripts

a	Ambient
g	Glass cover
w	Basin water
b	Basin liner

cover and runs down along the cover surface due to gravity and gets collected gradually in a beaker through condensate channel.

Various improved designs and modifications of a solar still have been made by several researchers all over the world to make the features attractive, improve the performance, feasibility and adaptability. A number of theoretical studies were also conducted. Dunkle [1] presented the heat equations of heat and mass transfer relations and empirical relations of convective and evaporative heat transfer coefficient for a single basin solar still. The calculation of glass cover temperature for a given ambient and basin water temperature was done using heat balance equations with the help of trial and error method. Lof et al. [2] analyzed the climatic and operational parameters on the various designs of solar still for improving the working and productivity. Morse and Read [3] developed the graphical method for determining the performance of a solar still by means of characteristic chart. Cooper [4,5] determined the maximum efficiency of single effect, horizontal solar stills and investigated the various parameters of still under transient operation with greenhouse effect by simulation technique. Experiments were carried out on the output of a solar still by using different dyes by Sodha et al. [6]. It was found

that black and violet dyes are more effective than other dyes for large basin water mass. Adhikari et al. [7] suggested that the Dunkle's relation was valid only when the Grashof number was less than 2.51×10^5 , but for the higher values of the Grashof number, presented a new relation for estimating the hourly distillate yield directly. Kumar and Tiwari [8] developed a theoretical thermal model to determine the convective mass transfer coefficient for different Grashof number ranges in solar distillation process. Based on linear regression analysis using experimental data, the values of c & n (unknown constants in the Nusselt number expression) have been calculated by software to predict the exact performance of a solar still for a different range of Grashof number.

Sakthivel et al. [9] conducted experiments and developed a mathematical model to improve the productivity of a conventional single slope solar still with jute cloth applied vertically in the middle of basin saline water and also attached to the rear wall of still in order to provide the large evaporation surface area. Srivastava and Agrawal [10] presented experimental and theoretical work and improved the performance of the conventional basin type solar still incorporating multiple low thermal inertia porous absorbers (blackened jute cloth) floated adjacent to each other on the basin water with the help of thermocol insulation. The result indicates that on clear days, about 68% more distillate output was obtained by the modified still. El-Sebaei et al. [11] fabricated a single basin single slope still with baffle suspended absorber and also developed a transient mathematical model for the solar still. Experimental and theoretical investigations were found that suspended absorbing plate divides the basin water into upper and lower portion. The daily productivity of modified still was increased by 18.5% to 20% compared to conventional still.

Naim et al. [12] fabricated non-conventional solar stills with charcoal particles as the absorbing medium. They found that charcoal particle granules acted as a good absorber medium than wick type absorber, black butyl rubber or asphalts. The productivity was 15% higher than that of wick type still. Nafey et al. [13] developed some methods to improve the productivity of single basin single slope solar still by using different absorbing material such as black rubber mat with the thickness of 2, 6 and 10 mm and black gravel with different sizes (7–12, 12–20 and 20–30). The experimental results showed that the solar still productivity was increased by 20% using black rubber (10 mm thick) and black gravel with sizes 20–30 mm increased the productivity by 19%.

Abdullah et al. [14] examined the effect of types of absorbing materials on various thermal performances of single basin single slope solar still. They used three absorbing materials such as uncoated metallic wiry sponge, coated metallic wiry sponge and black volcanic rocks in three identical single slope solar stills. The result showed that the productivity was enhanced by 28%, 43% and 60% respectively for coated and uncoated metallic wiry sponge and black volcanic rocks. El-Sebaei et al. [15] simulated a transient mathematical model for single slope single basin solar still with and without phase change material (PCM) under the basin liner of the still. A thin layer of stearic acid as a PCM was used beneath the basin liner to enhance the overnight distillate of the still. The performance of a solar still was investigated by computer simulation and found that daily productivity was about 9.005 (kg/m²/day) and daily efficiency of 84.3% with PCM and productivity was about 4.998 (kg/m²/day) without PCM.

Tiwari et al. [16] investigated to find an optimum inclination for the glass cover of a solar still for obtaining the maximum productivity. The result depicted that the optimum inclination under Delhi climate conditions in summer should be around 10° for maximum productivity and for winter, the optimum inclination should be as large as possible for maximum Yield. Velmurugan et al. [17] enhanced the productivity by the integration of fins at the basin of the still and found that the productivity increased

by 29.6%, 15.3% and 45.5% when wick, sponges and fins were used at the basin of the still respectively. Srivastava and Agrawal [18] performed an experimentation on modified single slope single basin solar still integrated with extended porous fins made up of blackened old cotton rags. The result showed that the maximum distillate output about 7.5 kg/m² was obtained in the month of May, which is 15% higher than conventional one. Omara et al. [19] conducted an experimental study and compared the performance of finned and corrugated still with the conventional still for same water quantity and same water depth. The result found that the productivity of finned and corrugated solar still was about 40% and 21% higher than conventional still respectively. Tanaka and Nakatake [20] proposed the theoretical analysis of a basin type solar still with internal and external reflectors and found that productivity of single basin single slope solar still was increased by 48% for the entire year. Setoodeh et al. [21] developed a three dimensional, two-phase model for evaporation and condensation processes in a single basin single slope solar still by using computational fluid dynamics (CFD) method and compared the predicted results with experimental data, and found that the computational fluid dynamics is a powerful tool for removing the problems during design, construction, experimentation and analysis of solar still.

The data on productivity and efficiency of solar still is dependent on the location of the place where experimentation is done. In order to assess the utility and feasibility of solar still in the central Indian location, experiments on single basin, single slope solar still were conducted and data obtained for productivity and efficiency of solar still. In this paper, the results obtained from the theoretical and the experimental study are compared and presented.

2. Experimentation

2.1. Experimental setup

The schematic diagram and experimental setup view of single basin single slope solar still is shown in Figs. 1 and 2. The solar still is designed and constructed to investigate the effect of different climatic and operating parameters under the same climatic condition of the middle part of India at Rewa (Latitude: 24°33' 20.81" N, Longitude: 81°18' 49.1" E). The solar still basin is fabricated by galvanized iron sheet (0.001 m thick) and it is shaped like a box with dimensions of 0.85 m length, 0.60 m breadth and 0.20 m height. The metallic basin box is contained in a plywood box. Plywood box consists of plywood (0.009 m thick) having four sides, two of these sides are rectangular in shape, while the other two sides are trapezoidal. Polystyrene sheet (0.005 m thick) is used for insulation between basin box and plywood frame in order to reduce the sides and bottom losses of heat transfer through four sides and base of the solar still system. The base of metallic box is painted black to enhance the capacity of solar radiation absorption. Three holes are made in solar still, one hole for feeding water inside the solar still and other two connect to the distillate water channel and drainage. A distillate channel is made by Aluminum sheet for collecting the distillate output through PVC pipe. It is set on the rectangular side edge of the solar still. Ordinary window glass (0.004 m thick) is used as a condensing surface. It is fixed completely on the edges of the wooden frame and a slope of 24° is given to the glass cover [16], which is almost equal to the latitude of Rewa. Silicone rubber and glass putty are used as a sealing material for filling the gap between the glass cover and solar still in order to prevent the vapor leakage. Plastic graduated bottle is used to collect the coming out distillate.

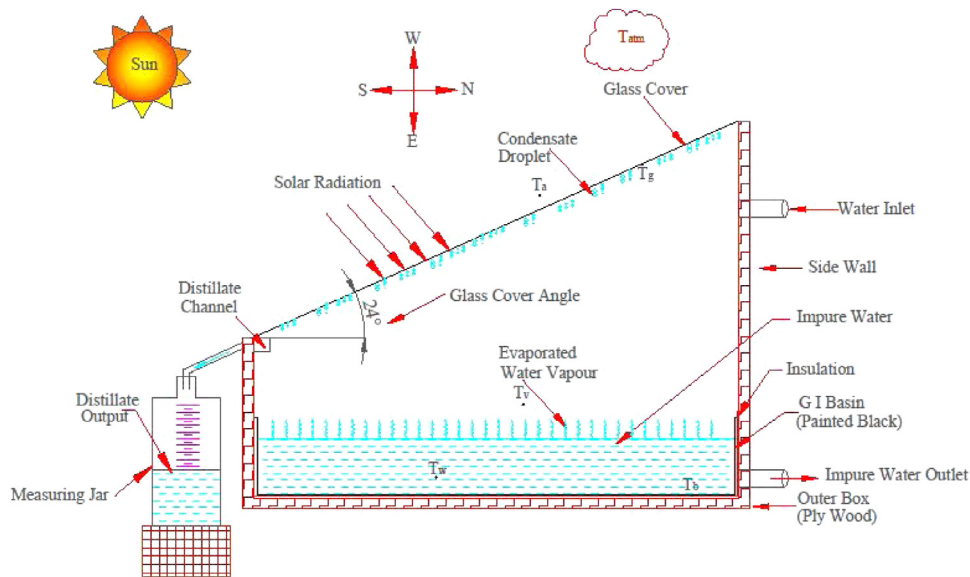


Fig. 1. Schematic diagram of single basin single slope solar still.

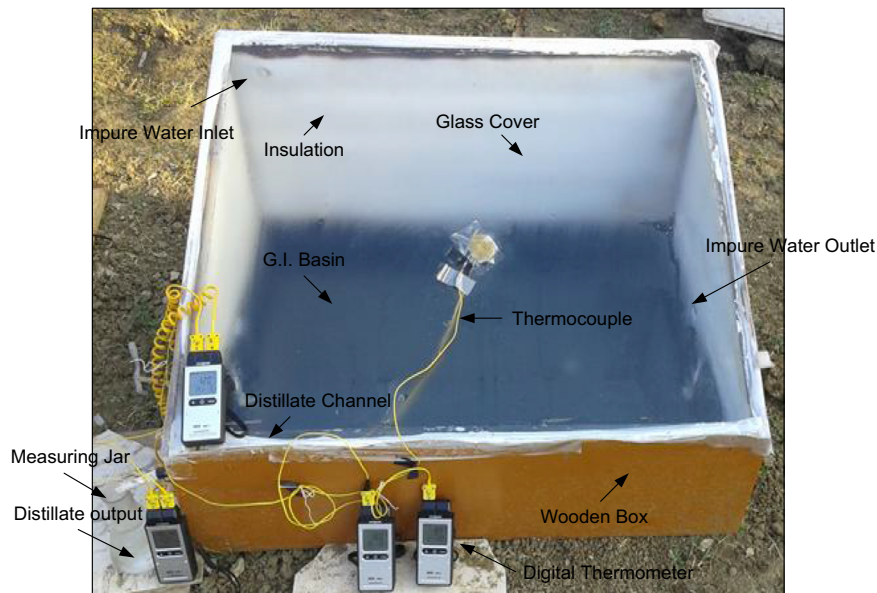


Fig. 2. Photograph of single basin single slope solar still.

2.2. Operational parameters

Global solar radiation and wind speed data are taken by the SRRA (Solar radiation resource assessment) station at the Rewa Engineering College, Rewa, Madhya Pradesh, India. It is installed by C-WET (Centre for Wind Energy Technology) Chennai, India, which is an autonomous organization of ministry of new and renewable energy, Government of India. Temperature is measured by calibrated Ni-Cr thermocouples connected with multichannel digital thermometer at various points of solar still, viz, basin water temperature (T_w), glass cover temperature (T_g), basin liner temperature (T_b) and vapor temperature (T_v). Ambient air temperature is measured by thermometer. Experiments were conducted at Rewa, M. P., India in the month of May, 2016. The solar still is placed in north-south direction with the condensing cover inclination facing south in order to maximize the receiving of solar radiation. The solar still basin is filled with underground water (TDS value of

1043 mg/ml) collected from Rewa Engineering College, Rewa. The experiments are carried out in a solar still for five different water depths (2,4,6,8,10 cm) for five consecutive days. The collection of distillate and all the required readings of the still are recorded every hour from 7:00 a.m. to 7:00 a.m. the next morning. In Fig. 4 various parameters are plotted against time starting from 7:00 a.m. The numbers from 25 to 31 on the time axis of this plot indicate time from 1:00 a.m. to 7:00 a.m. of the next morning for correct representation on the graph. In this way, the observations for 24 h were recorded and the nocturnal output was also considered. The starting time is indicated by 7:00 a.m. in the graph (Fig. 4).

Range of solar intensity is taken as 0.0 W/m^2 – 915.0 W/m^2 and that of wind velocity is taken as 0.25 m/s – 5.0 m/s based on actual data available from SRRA station at Rewa. Values of basin water temperature, glass temperature, basin liner temperature and ambient air temperature were measured directly and the same were used in the theoretical calculations.

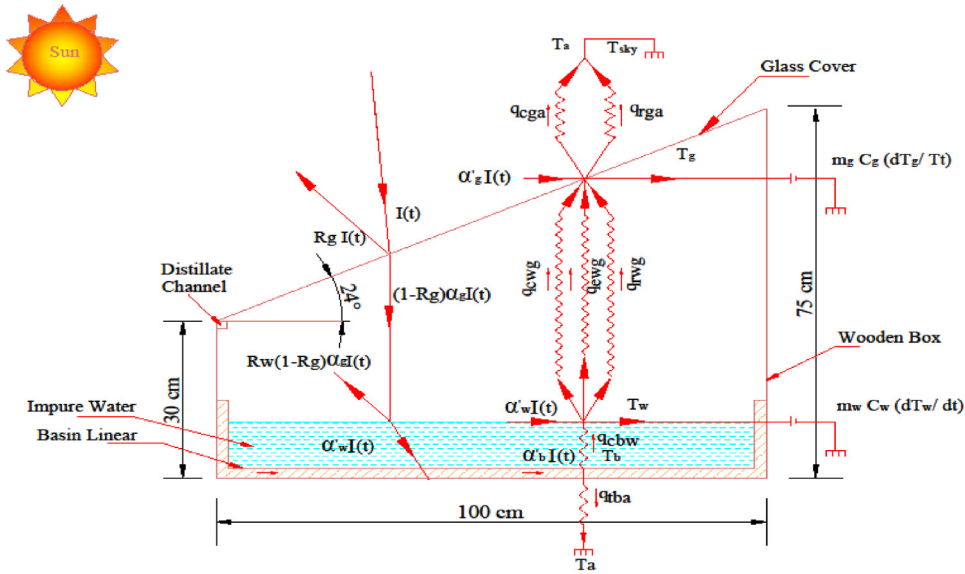


Fig. 3. Schematic diagram of heat transfer analogy of single basin single slope solar still.

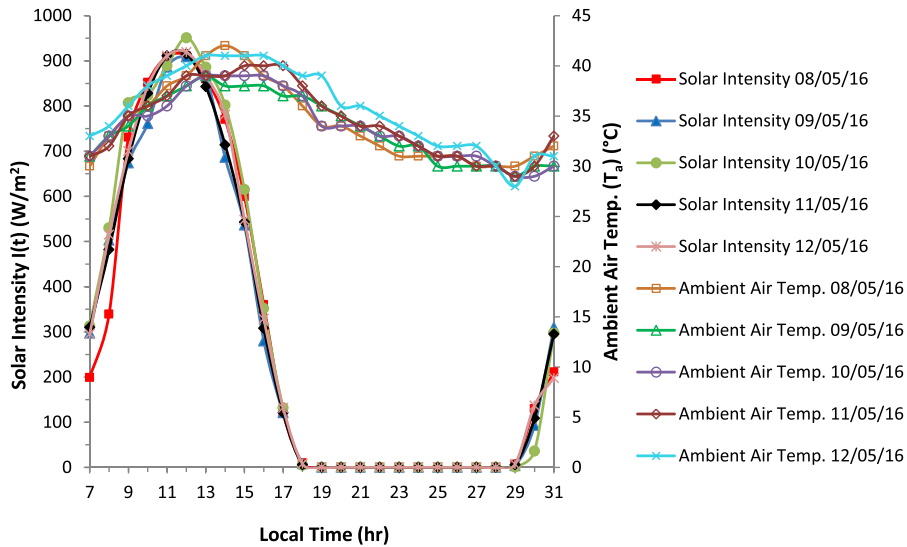


Fig. 4. Hourly variation of solar intensity and ambient air temperature on a (7:00 a.m. to 7:00 a.m. the next morning) typical summer day.

3. Thermal energy calculations of solar still model

In order to simplify the thermal energy balance equations for various parts of a single basin single slope solar still, the following assumptions have been made:

- Heat capacity of condensing cover and insulating materials (sides and bottom) is negligible as compared to the basin water.
- Solar still is assumed as a perfect vapor leakage proof unit.
- Water vapor and dry air are assumed to behave like an ideal gas.
- The physical properties of water used in experiments remain constant with different temperature range.

Thermal modeling of solar still is the set of the mathematical equations of energy transfer at the various points of the system. Solar distillation system design can be efficiently analyzed for many parameters by using thermal modeling with less resources of money and time.

3.1. The following energy balance equations [22] are written for thermal modeling of conventional solar still for various parts such as glass cover, water mass and basin liner

3.1.1. Glass cover

The heat is received by the glass cover from incident solar radiation as a fraction of total solar radiation and basin water surface (Convection, evaporation and radiation) and rejected by the glass cover to the atmosphere through convection and radiation,

$$\alpha'_g I(t) + q_{twg} = q_{tga} \tag{3.1}$$

where,

$$q_{twg} = q_{cwg} + q_{ewg} + q_{rwg} \tag{3.2}$$

$$q_{tga} = q_{cga} + q_{rga} \tag{3.3}$$

$$\alpha'_g I(t) + h_{twg}(T_w - T_g) = h_{tga}(T_g - T_a) \tag{3.4}$$

3.1.2. Basin water mass

Heat energy is absorbed by the basin water due to fraction of transmitted solar radiation striking on it and it is absorbed by water from basin liner. Absorbed heat energy is consumed in two ways, one part is stored in water due to its specific heat and remaining part of heat energy is transferred from water surface to the glass cover by convection, evaporation and radiation,

$$\alpha'_w I(t) + q_{cbw} = q_{twg} + m_w C_w (dT_w/dt) \tag{3.5}$$

$$\alpha'_w I(t) + h_{cbw}(T_b - T_w) = h_{twg}(T_w - T_g) + m_w C_w (dT_w/dt) \tag{3.6}$$

3.1.3. Basin liner

Heat energy is absorbed by basin liner due to fraction of transmitted solar radiation striking on it and it is released by basin liner to basin water and remaining heat is lost from basin liner to atmosphere through the bottom and sides of the solar still by conduction and convection,

$$\alpha'_b I(t) = q_{cbw} + q_{tba} \tag{3.7}$$

$$\alpha'_b I(t) = h_{cbw}(T_b - T_w) + h_{tba}(T_b - T_a) \tag{3.8}$$

Substituting the value of T_g and T_b from Eqs. (3.4) and (3.8) in Eq. (3.6) and solving we get,

$$(dT_w/dt) + a T_w = f(t) \tag{3.9}$$

where,

$$a = U_L / (m_w C_w)$$

$$f(t) = M I(t) + N T_a$$

$$M = (\alpha'_{eff} h_{cbw}) / m_w C_w (h_{cbw} + h_{tba})$$

$$N = U_L / (m_w C_w)$$

The solution of Eq. (3.9) is written as,

$$T_w = (\bar{f}(t)/a)(1 - e^{-at}) + T_{w0} e^{-at} \tag{3.10}$$

where, T_{w0} is the temperature of basin water at ($t=0$) and $\bar{f}(t)$ is the average value of $f(t)$ for the time interval between 0 and t .

Now the rate of evaporative heat loss is given by,

$$q_{ewg} = h_{ewg}(T_w - T_g) \tag{3.11}$$

And the hourly distillate per unit basin area is obtained from the relation,

$$M_w = (h_{ewg}(T_w - T_g) \times 3600) / (L_{ev}) \tag{3.12}$$

Daily distillate per unit basin area is given as,

$$M'_w = \sum_{i=1}^{24} M_w \tag{3.13}$$

The efficiency of the solar still is given by the relation,

$$\eta = \frac{M'_w \times L_{ev}}{A_b \times \sum I(t) \times \Delta t} \tag{3.14}$$

3.2. Internal and external heat transfer analogy of the solar still is shown in Fig. 3. There are mainly two types of heat transfers taking place in the process of solar still

3.2.1. Internal heat transfer process

The internal heat transfer takes place from the basin water to the inner surface of glass cover through the three modes of convection, evaporation and radiation by which the internal heat transfer process is governed in distillation unit.

The convective heat transfer occurs between basin water surface and inner side of the glass cover. It is calculated by the following equation,

$$q_{cwg} = h_{cwg}(T_w - T_g) \tag{3.15}$$

where, the convective heat transfer coefficient is obtained from an empirical relation, which is given by Dunkle [1].

$$h_{cwg} = 0.884 \left[(T_w - T_g) + \frac{(P_w - P_g)(T_w + 273)}{(268.9 \times 10^3 - P_w)} \right]^{1/3} \tag{3.16}$$

The evaporative heat transfer occurs between the water surface and glass cover in the form of the water to the air-vapor mixture (humid air),

$$q_{ewg} = h_{ewg}(T_w - T_g) \tag{3.17}$$

where, the evaporative heat transfer coefficient between water and glass cover is found from [23].

$$h_{ewg} = (16.28 \times 10^{-3}) h_{cwg} (P_w - P_g) / (T_w - T_g) \tag{3.18}$$

The radiative heat transfer occurs between any two bodies which are at different temperature. In this case the water surface and glass cover are considered as infinite parallel planes [24]. The radiative heat transfer from water surface to the glass cover is given by:

$$q_{rwg} = h_{rwg}(T_w - T_g) \tag{3.19}$$

Also the radiative heat transfer given by Stefan Boltzman's equation is given below,

$$q_{rwg} = \epsilon_{eff} \sigma [(T_w + 273)^4 - (T_g + 273)^4] \tag{3.20}$$

where ϵ_{eff} is the effective emissivity of water surface to the glass cover and σ is the Stefan Boltzman's constant taken as $5.67 \times 10^{-8} \text{ W/m}^2\text{K}^4$. From the Eqs. (3.19) and (3.20) we get,

$$h_{rwg} = \epsilon_{eff} \sigma [(T_w + 273)^4 - (T_g + 273)^4] / (T_w - T_g) \tag{3.21}$$

Total internal heat transfer coefficient of water surface to the inner surface of the glass cover is the sum of these entire heat transfer coefficients by all these modes thus,

$$h_{twg} = h_{cwg} + h_{ewg} + h_{rwg} \tag{3.22}$$

3.2.2. External heat transfer process

External heat losses are contributed by the top losses, bottom losses and side losses of the solar still.

3.2.2.1. Top loss coefficient. In order to provide the minimum thickness of glass cover for obtaining the uniform temperature on it, the radiative and convective losses from the glass cover to the external atmosphere can be written as [25].

$$q_{tga} = q_{rga} + q_{cga} \tag{3.23}$$

where,

$$q_{rga} = h_{rga}(T_g - T_{sky}) \tag{3.24}$$

$$q_{rga} = \epsilon_g \sigma [(T_g + 273)^4 - (T_{sky} + 273)^4] \tag{3.25}$$

where,

$$h_{rga} = \varepsilon_g \sigma \left[(T_g + 273)^4 - (T_{sky} + 273)^4 \right] / (T_g - T_{sky}) \quad (3.26)$$

where, the sky temperature is estimated from [26].

$$T_{sky} = 0.0552 \times T_a^{1.5} \quad (3.27)$$

$$q_{cga} = h_{cga}(T_g - T_a) \quad (3.28)$$

where, [27,28]

$$(a) h_{cga} = 2.8 + 3.0V_w \text{ if } V_w \leq 5 \text{ m/s} \ \& \ 6.15 \times (V_w)^{0.8} \text{ if } V_w > 5 \text{ m/s.}$$

$$(b) h_{cga} = 5.7 + 3.8V_w \text{ if } V_w > 5 \text{ m/s.}$$

The total heat loss coefficient from the glass cover to the outer atmosphere,

$$h_{tga} = h_{rga} + h_{cga} \quad (3.29)$$

3.2.2.2. Bottom and side loss coefficient. Heat is lost from the water in the basin to the outer atmosphere through the insulation on the bottom and sides of the basin and modes of heat loss are conduction, evaporation and radiation. Therefore, the heat loss equation for the bottom is written as,

$$q_{tba} = h_{tba}(T_b - T_a) \quad (3.30)$$

where, the heat loss coefficient from basin liner to the atmosphere is given as [34],

$$h_{tba} = [(L_i/K_i) + (1/h_{ba})]^{-1} \quad (3.31)$$

where,

$$h_{ba} = h_{rba} + h_{cba} \quad (3.32)$$

Side heat loss can be given as,

$$h_{sa} = h_{tba} \times (A_s/A_b) \quad (3.33)$$

If the side area of still (A_s) is very small and compared with basin liner area of still (A_b) then side heat loss coefficient can be neglected.

3.3. The fraction of solar radiation at various parts of solar still [22,29]

Fraction of solar radiation absorbed by a glass cover,

$$\alpha'_g = (1 - R_g)\alpha_g \quad (3.34)$$

Fraction of solar radiation absorbed by water,

$$\alpha'_w = (1 - \alpha_g)(1 - R_g)(1 - R_w)\alpha_w \times (\text{Without attenuation factor}) \quad (3.35)$$

$$\alpha'_w = (1 - \alpha_g)(1 - R_g)(1 - R_w) \times [1 - \sum \mu_j \text{EXP}(-\eta_j d_w)] \times (\text{With attenuation factor}) \quad (3.36)$$

Fraction of solar radiation absorbed by basin liner,

$$\alpha'_b = \alpha_b(1 - \alpha_g)(1 - R_g)(1 - \alpha_w)(1 - R_w) \times (\text{Without attenuation factor}) \quad (3.37)$$

$$\alpha'_b = \alpha_b(1 - \alpha_g)(1 - R_g)(1 - R_w) \times [\sum \mu_j \text{EXP}(-\eta_j d_w)] \times (\text{With attenuation factor}) \quad (3.38)$$

where, $\sum \mu_j \text{EXP}(-\eta_j d_w)$ is the attenuation factor and depends on different lengths, which is shown in Table 1(a) and (b).

Table 1a

[22]. The values of μ_j (Fraction of solar flux having extinction coefficient) and η_j (Extinction coefficient).

J	μ_j	η_j (m ⁻¹)
1	0.237	0.032
2	0.193	0.45
3	0.167	3.0
4	0.179	35.0
5	0.124	225.0

Table 1b

Variation of attenuation factor with water depth (d_w).

d_w (m)	$\sum \mu_j \text{EXP}(-\eta_j d_w)$
0.02	0.6756
0.04	0.6185
0.06	0.5858
0.08	0.5648
0.10	0.5492

Table 2

Ranges, accuracies and errors for various measuring instruments used in the experiments.

Sl. No.	Instrument	Range	Accuracy	% Error
1	Thermometer	0–100 °C	±1 °C	±0.5%
2	Thermocouple	–100–200 °C	±0.1 °C	±0.25%
3	Pyranometer	0–1000 W/m ²	±1 W/m ²	±1%
4	Anemometer	0–25 m/s	±0.1 m/s	±5%
5	Measuring beaker	0–500 ml	±2 ml	±2%

4. Experimental error analysis

Performance evaluation of solar still is based on several parameters used in the experimentation. These measured parameters generally include some errors due to the uncertainty of method of measurement and limited precision of the experimental instruments. These errors, known as total percentage of uncertainty, may affect the accuracy of results. The minimum error occurred in an instrument is equal to ratio between its least count and minimum value of the output measured [30]. Thermometer, thermocouple, pyranometer, anemometer and measuring beaker are used for measuring the ambient temperature, basin water temperature, glass temperature, basin liner temperature, global solar radiation, wind velocity, and amount of distillate output. The ranges, accuracies, and percentage errors of these instruments are given in Table 2. The total percentage of uncertainty of experimental measurement has been calculated by using the procedure explained by Holman [31] and found to be within ±10%.

5. Results and discussion

The experimentation was conducted for five days having five different basin water depths of ground water on single basin single slope solar still under the typical summer climatic condition in Rewa, India. Major precautions were taken during conduction of experiments to get the data as accurate as possible. For theoretical calculation, thermal model is prepared by a set of mathematical equations and solved by the computer program on Excel software. After that the results of theoretical thermal model are validated by comparing them with corresponding experimental results obtained from the present work. For present theoretical model, set of design parameters are given in Table 3. Theoretical and exper-

Table 3
Physical input design parameters of the single basin single slop solar still.

Sl. No.	Relevant parameters	Numerical values
1	α_g [32]	0.05
2	α_w [32]	0.05
3	α_b [32]	0.90
4	R_g [32]	0.05
5	R_w [32]	0.05
6	ε_g [33]	0.94
7	ε_w [33]	0.95
8	ε_{eff} [33]	0.82
9	C_w [32]	4180 J/kg°C
10	A_b	1 m ²
11	t_g	0.004 m
12	K_i	0.033 W/m°C
13	L_i	0.010 m
14	σ	5.6697×10^{-8} W/m ² K ⁴
15	h_{ba} [34]	2.8 W/m ² °C
16	h_{cbw} [34]	250 W/m ² °C (Summer)
17	t	3600 s

imental results obtained from the present work in summer days are presented, validated and discussed in the following sections.

5.1. Variation of solar intensity and ambient air temperature

Tables 4 and 5 show the hourly variation of global solar intensity (Experimental) and wind velocity (Experimental) for five typical days of summer season. Fig. 4 clearly depicts the hourly variation of the received solar intensity on the solar still and ambient air temperature for five different depths during five continuous days of the summer season. It can be observed that the maximum value of solar intensity is reached at mid noon and thereafter it begins to decrease up to the evening, whereas the ambient air temperature is reached to the maximum value at 3:00 p.m. The maximum value of solar intensity is attained faster than the maximum value of ambient air temperature mainly due to more thermal capacity of ambient air. As shown in the figure, the trend of the graph of solar intensity for five days is more or less similar and the maximum value is obtained on May 10, 2016

(6 cm water depth) at mid noon while the trend of the graph of ambient air temperature for five days varies slightly throughout the day and maximum value is obtained on May 8, 2016 (2 cm water depth) at around 3:00 p.m.

5.2. Hourly variation of basin water temperature with depth of basin water

Hourly variation of theoretical and experimental values of basin water temperature for different water depths has been shown in the Fig. 5. It is clearly observed that, the maximum value of basin water temperature decreases with an increase in the depth of basin water significantly. It is due to high thermal inertia of the higher depth of basin water mass. The theoretical and experimental values of maximum basin water temperatures are 88 °C and 73 °C respectively at around 13:00 h for minimum basin water depth (2 cm) while for the maximum basin water depth (10 cm), the values of maximum basin water temperatures are 65 °C and 62 °C respectively at around 15:00 h. Due to increase in basin water depth, the maximum value of basin water temperature is shifted towards afternoon hours and this high temperature is also retained in the evening. This results in a slight decrease in day hour output and increase in nocturnal output. It is clearly seen that the theoretical and experimental values of basin water temperature show a good agreement.

5.3. Hourly variation of glass cover and basin liner temperature with depth of basin water

Fig. 6 clearly shows that the hourly variation of theoretical and experimental values of outer side of glass cover temperature for different basin water depths. It is observed that the theoretical outer glass cover temperature is closer to the experimental values of outer glass cover temperature for different basin water depths. Morning and evening outer glass cover temperature attained with the low basin water depth is lesser than the temperature with high basin water depth. Fig. 7 illustrates the hourly variation of theoretical and experimental values of basin liner temperature. It is clearly noticed that the lowest basin water depth attains the highest basin water temperature and it decreases with an increase

Table 4
Hourly variation of global solar intensity (Experimental) for five typical days of summer season.

Sl No.	Time (h)	Solar intensity (W/m ²) 08/05/16	Solar intensity (W/m ²) 09/05/16	Solar intensity (W/m ²) 10/05/16	Solar intensity (W/m ²) 11/05/16	Solar intensity (W/m ²) 12/05/16
1	07:00–8:00	199	297	313	310	295
2	08:00–9:00	339	503	530	482	515
3	09:00–10:00	731	674	807	683	700
4	10:00–11:00	852	761	823	828	844
5	11:00–12:00	909	886	889	911	911
6	12:00–13:00	911	909	951	915	919
7	13:00–14:00	860	867	886	843	867
8	14:00–15:00	770	686	802	714	781
9	15:00–16:00	599	536	615	543	548
10	16:00–17:00	360	280	352	308	329
11	17:00–18:00	121	121	132	121	132
12	18:00–19:00	10	8	5	6	8
13	19:00–20:00	0	0	0	0	0
14	20:00–21:00	0	0	0	0	0
15	21:00–22:00	0	0	0	0	0
16	22:00–23:00	0	0	0	0	0
17	23:00–24:00	0	0	0	0	0
18	24:00–01:00	0	0	0	0	0
19	01:00–02:00	0	0	0	0	0
20	02:00–03:00	0	0	0	0	0
21	03:00–04:00	0	0	0	0	0
22	04:00–05:00	0	0	0	0	0
23	05:00–06:00	7	4	1	6	7
24	06:00–07:00	130	93	110	109	137

Table 5
Hourly variation of wind velocity for five typical days of summer season.

Sl No.	Time (h)	Wind velocity (m/s) 08/05/16	Wind velocity (m/s) 09/05/16	Wind velocity (m/s) 10/05/16	Wind velocity (m/s) 11/05/16	Wind velocity (m/s) 12/05/16
1	07:00–8:00	1.30	0.83	1.89	4.48	1.26
2	08:00–9:00	1.51	1.88	1.88	2.95	3.71
3	09:00–10:00	1.99	2.10	2.03	2.73	1.91
4	10:00–11:00	1.34	1.98	2.27	2.66	3.29
5	11:00–12:00	0.81	1.49	3.40	4.74	2.17
6	12:00–13:00	1.61	2.31	3.70	4.63	1.34
7	13:00–14:00	2.46	1.98	2.50	2.10	2.34
8	14:00–15:00	4.02	3.09	4.30	4.45	4.10
9	15:00–16:00	1.12	1.89	2.75	1.15	2.87
10	16:00–17:00	1.86	1.54	2.21	0.83	4.10
11	17:00–18:00	2.33	1.83	1.61	0.26	2.87
12	18:00–19:00	1.80	1.69	1.36	1.65	4.10
13	19:00–20:00	1.31	4.38	1.64	1.89	2.31
14	20:00–21:00	1.51	3.00	2.67	1.79	3.10
15	21:00–22:00	0.73	2.43	2.33	1.54	2.00
16	22:00–23:00	2.14	3.14	1.80	1.16	2.41
17	23:00–24:00	3.17	2.87	1.99	3.18	1.51
18	24:00–01:00	2.76	3.08	2.03	3.37	2.26
19	01:00–02:00	1.11	2.98	0.85	0.84	1.22
20	02:00–03:00	1.14	2.44	0.41	3.35	1.12
21	03:00–04:00	0.85	4.22	0.42	2.59	1.32
22	04:00–05:00	2.68	2.47	0.68	2.55	0.88
23	05:00–06:00	2.61	3.36	0.72	3.20	1.38
24	06:00–07:00	2.02	3.16	0.37	3.35	0.98

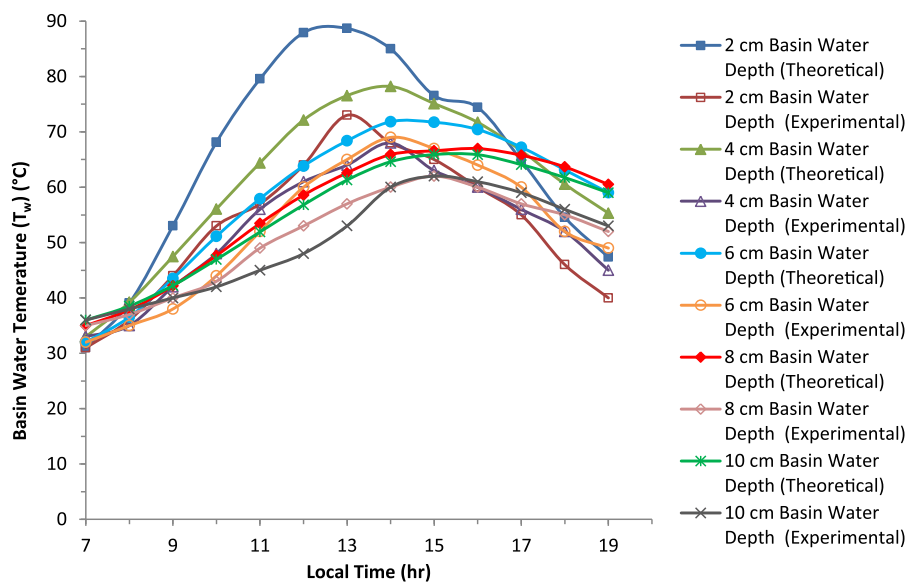


Fig. 5. Hourly variation of theoretical and experimental values of basin water temperature with different basin water depths of solar still in May 2016.

of basin water depth. There is a good agreement between theoretical values and experimental values of basin liner temperature.

5.4. Hourly variation of heat transfer coefficients for different basin water depths

Figs. 8–12 clearly depict the hourly variation of theoretical values and experimental values of heat transfer coefficients (due to evaporation, convection and radiation) from basin water to glass cover in single basin single slope solar still. The evaporative heat transfer coefficient increases with time and achieves the maximum value between 13:00 h to 15:00 h for all basin water depths from 2 cm to 10 cm. After 15:00 h, its value decreases with time for both the cases (theoretical and experimental). The maximum theoretical and experimental values of evaporative heat transfer coefficients are obtained as $54 \text{ W/m}^2 \text{ }^\circ\text{C}$ and $42 \text{ W/m}^2 \text{ }^\circ\text{C}$ respectively, at 2 cm basin water depth, and minimum values are

obtained as $32 \text{ W/m}^2 \text{ }^\circ\text{C}$ and $26 \text{ W/m}^2 \text{ }^\circ\text{C}$ respectively at 10 cm basin water depth. This is due to the fact that the quantity of basin water of solar still increases with an increase in basin water depth so that the thermal inertia of water increases and the rate of evaporation of the water decreases and as a result, the time of achieving the maximum value of the evaporative heat transfer coefficient is shifted from 13:00 h to 15:00 h for increasing basin water depth from 2 cm to 10 cm. It is further noted from these figures that the theoretical and experimental values of convective and radiative heat transfer coefficients are much lesser than the value of the evaporative heat transfer coefficient. The maximum theoretical and experimental values of convective heat transfer coefficients are obtained as $2.7 \text{ W/m}^2 \text{ }^\circ\text{C}$ and $2.15 \text{ W/m}^2 \text{ }^\circ\text{C}$ respectively at 2 cm basin water depth. The maximum theoretical and experimental values of radiative heat transfer coefficients are obtained as $8.6 \text{ W/m}^2 \text{ }^\circ\text{C}$ and $7.6 \text{ W/m}^2 \text{ }^\circ\text{C}$ respectively at 2 cm basin water depth. For 10 cm basin water depth, the corresponding

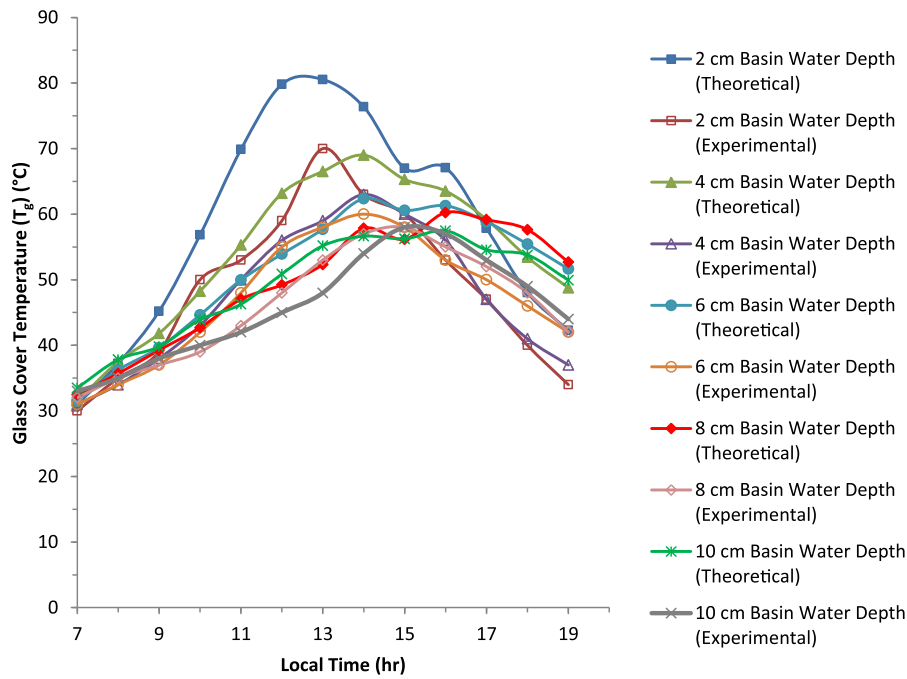


Fig. 6. Hourly variation of theoretical and experimental values of glass cover temperature with different basin water depths of solar still in May 2016.

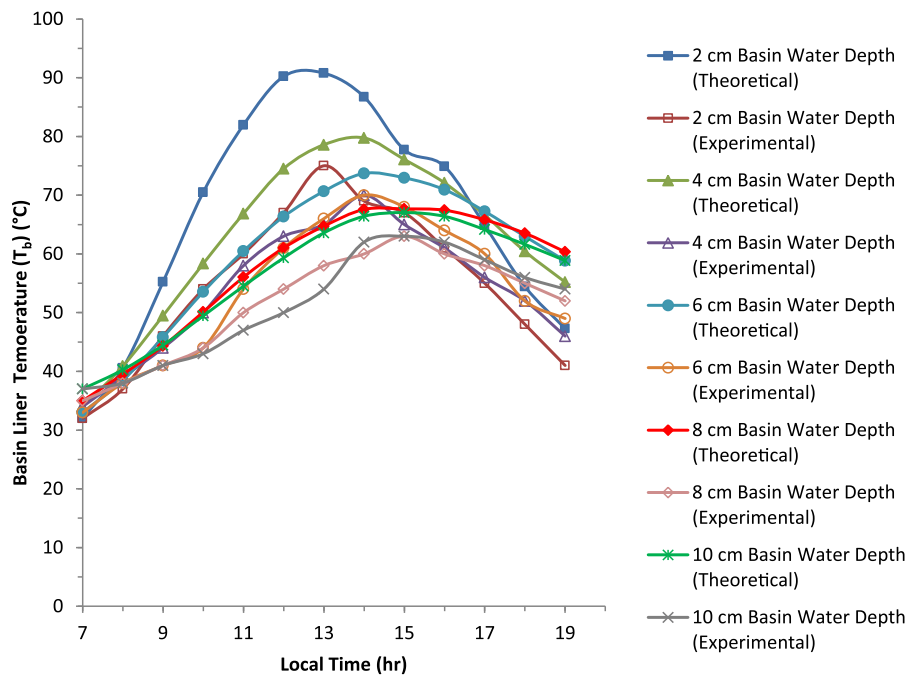


Fig. 7. Hourly variation of theoretical and experimental values of basin liner temperature with different basin water depths of solar still in May 2016.

values are $2.3 \text{ W/m}^2 \text{ }^\circ\text{C}$, $2.0 \text{ W/m}^2 \text{ }^\circ\text{C}$, $7 \text{ W/m}^2 \text{ }^\circ\text{C}$ and $6.8 \text{ W/m}^2 \text{ }^\circ\text{C}$ respectively. It is clearly observed that the pattern of experimental graph is very close to the theoretical graph, which shows a good agreement between the theoretical and experimental values of heat transfer coefficients for single basin single slope solar still.

5.5. Hourly variation of distillate output for different basin water depths

Fig. 13 shows the comparison of hourly variation of theoretical and experimental values of distillate output for different depths. The maximum distillate output is obtained from lower basin

water depth (2 cm) and minimum from higher basin water depth (10 cm). It can be observed that the amount of distillate output is inversely proportional to the basin water depth. This is caused by the higher rate of evaporation (due to high rise in temperature) for lower basin water depth. Therefore, distillate output decreases with increase in basin water depth in solar still. For 2 cm basin water depth, maximum theoretical and experimental values of distillate output are obtained as 830 gm/m^2 and 742 gm/m^2 respectively, at approx. 14:00 h. For 10 cm basin water depth, maximum theoretical and experimental values of distillate output are obtained as 395 gm/m^2 and 300 gm/m^2 respectively, at approx. 15:00 h. Nocturnal output is increased with increasing basin water

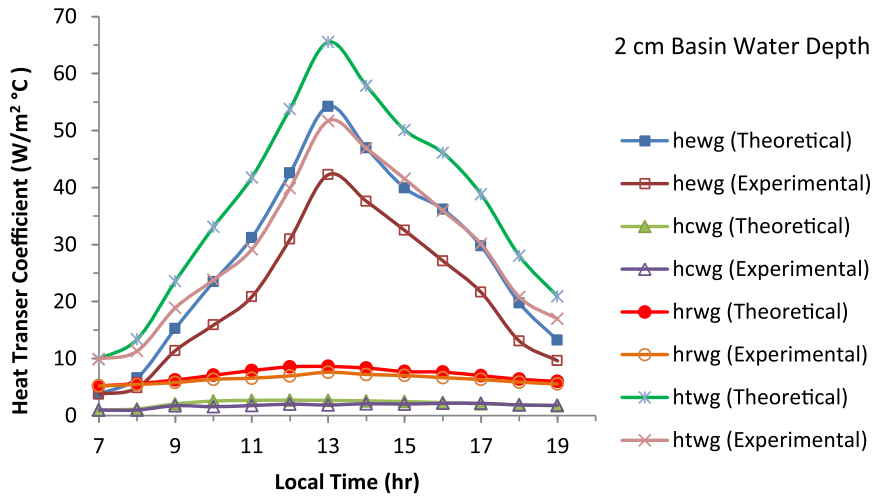


Fig. 8. Hourly variation of theoretical and experimental values of heat transfer coefficients of basin water to glass cover for 2 cm basin water depth.

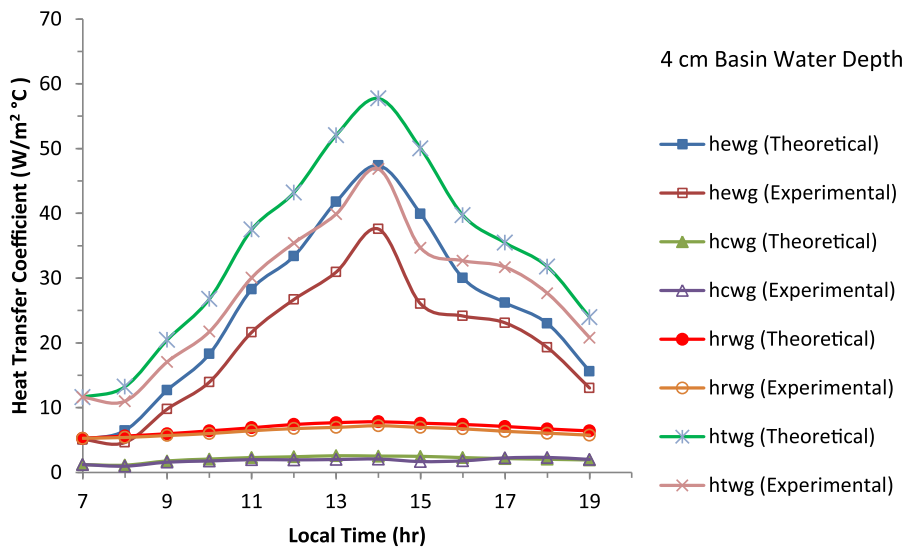


Fig. 9. Hourly variation of theoretical and experimental values of heat transfer coefficients of basin water to glass cover for 4 cm basin water depth.

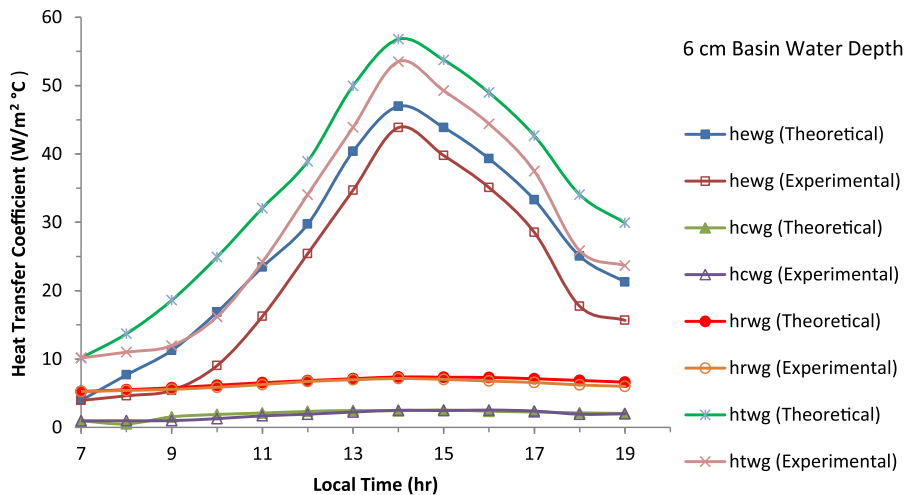


Fig. 10. Hourly variation of theoretical and experimental values of heat transfer coefficients of basin water to glass cover for 6 cm basin water depth.

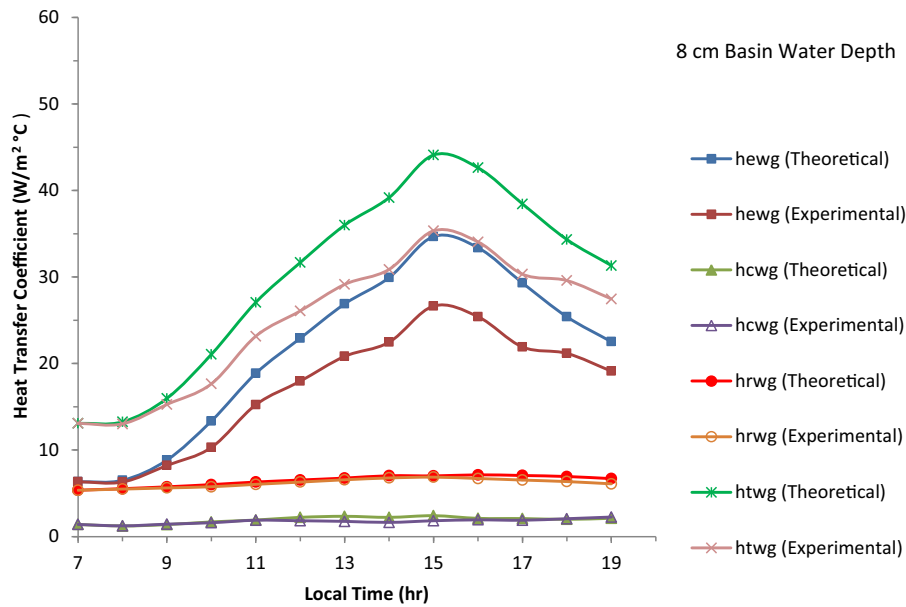


Fig. 11. Hourly variation of theoretical and experimental values of heat transfer coefficients of basin water to glass cover for 8 cm basin water depth.

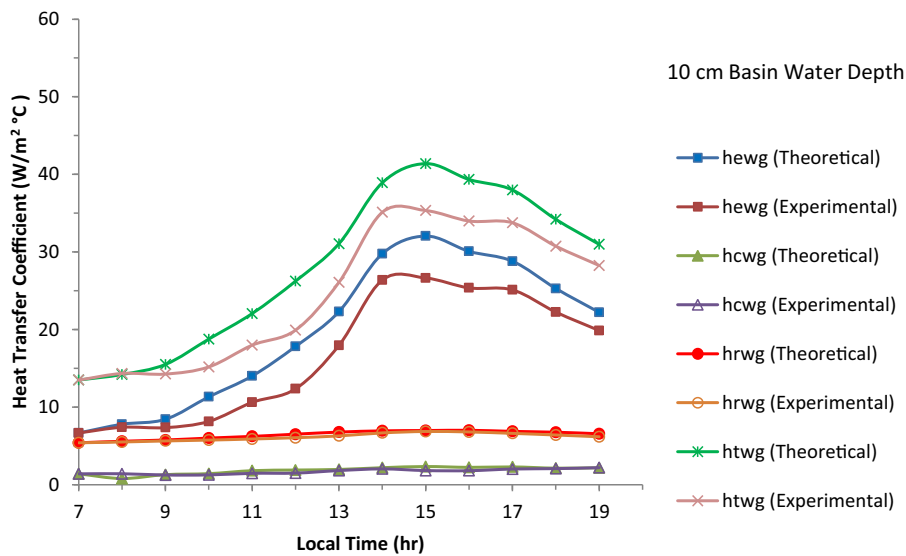


Fig. 12. Hourly variation of theoretical and experimental values of heat transfer coefficients of basin water to glass cover for 10 cm basin water depth.

depth due to release of more amount of heat thereby increasing the evaporation.

5.6. Comparison of theoretical and experimental values of distillate output

Fig. 14 shows the comparison of hourly variation of theoretical and experimental values of cumulative distillate output for 24 h (7 a.m. to 7 a.m. the next morning) for different basin water depths. The cumulative distillate output decreases with an increase of basin water depth of solar still. At 2 cm basin water depth of solar still, theoretical and experimental distillate output was 29% and 23% higher than that for the 10 cm basin water depth. This proves that the theoretical and experimental values of distillate output have good agreement. The theoretical and experimental amount of cumulative distillate output for 24 h at lowest basin water depth (2 cm) is approximately 5.37 kg/m²/d and 4.26 kg/m²/d

respectively. For highest basin water depth (10 cm), the theoretical and experimental amount of cumulative distillate output is approximately 4.17 kg/m²/d and 3.24 kg/m²/d respectively.

Fig. 15 depicts the theoretical and experimental values of distillate output of the solar still at day and night for different basin water depths. It has been observed that the nocturnal distillate output is also obtained in good amount when the basin water depth is increased. The reason behind this may be that, as the basin water depth is increased, the amount of water is also increased, so the amount of heat absorbed is increased over the daylight. Therefore, the water remains hot for long period of night resulting in a higher distillate output of a solar still. Theoretical and experimental values of nocturnal cumulative distillate output obtained for 10 cm basin water depth are 86% and 75% higher than those for 2 cm basin water depth of solar still.

Fig. 16 shows the daily distillate output of a solar still theoretically and experimentally for different basin water depths.

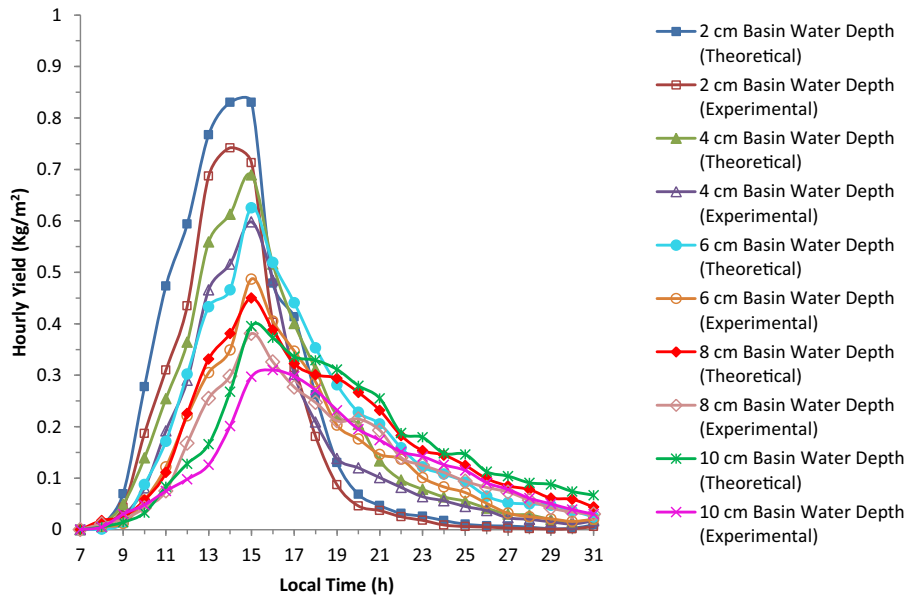


Fig. 13. Hourly variation of theoretical and experimental values of distillate output with different basin water depths of solar still in May 2016.

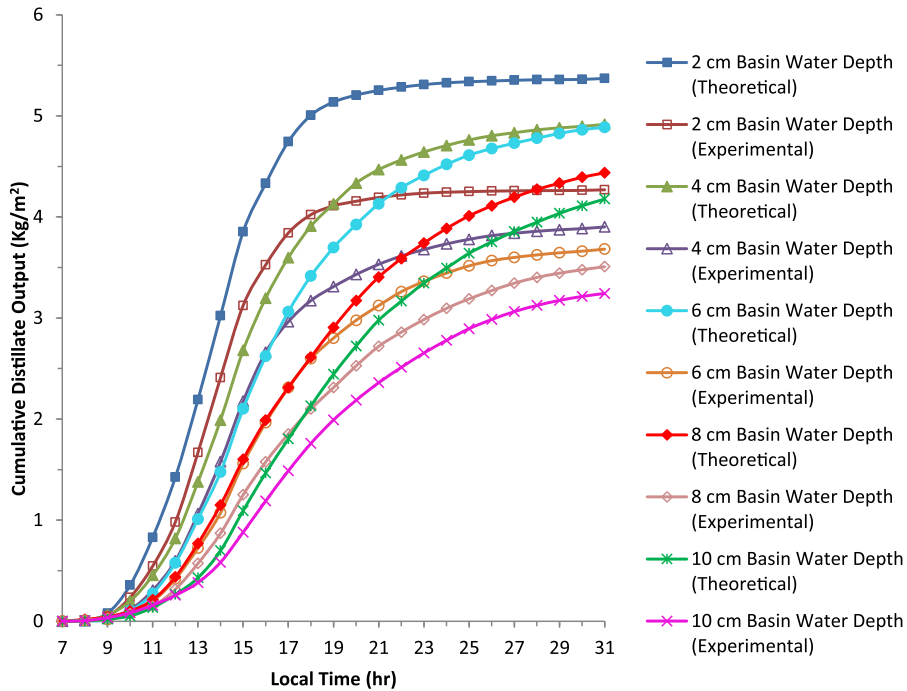


Fig. 14. Comparison of theoretical and experimental values of cumulative distillate output for 24 h (7 a.m. - 7 a.m. the next morning) with different basin water depths of solar still in May 2016.

Theoretical daily distillate output is higher than the experimental values at all basin water depths. The distillate output is decreased as the basin water depth increased. This proves that, lower basin water depth has a good effect on the distillate output of the still.

5.7. Comparison of theoretical and experimental daily efficiency of solar still

Fig. 17 illustrates the theoretical and experimental daily efficiency of a solar still for different water depths. The experimental value of daily efficiency is slightly lesser than the theoretical value, which shows the fair agreement between theoretical and experimental results. The daily efficiency is decreased as the basin

water depth is increased. The reason behind this may be that, the water temperature is quickly rising for a lower basin water depth due to minimum volume of water and gives the higher amount of productivity, therefore daily efficiency is greater than that for the higher value of basin water depth. The maximum and minimum values of daily efficiency are obtained at 2 cm and 10 cm basin water depth respectively. For 2 cm basin water depth, theoretical and experimental daily efficiency is around 52.83% and 41.99%, respectively, and for 10 cm basin water depth, the values are 41.75% and 32.42% respectively. Experimental efficiency is lower than the theoretical due to possible leakage of vapor as the vapor pressure of water increases.

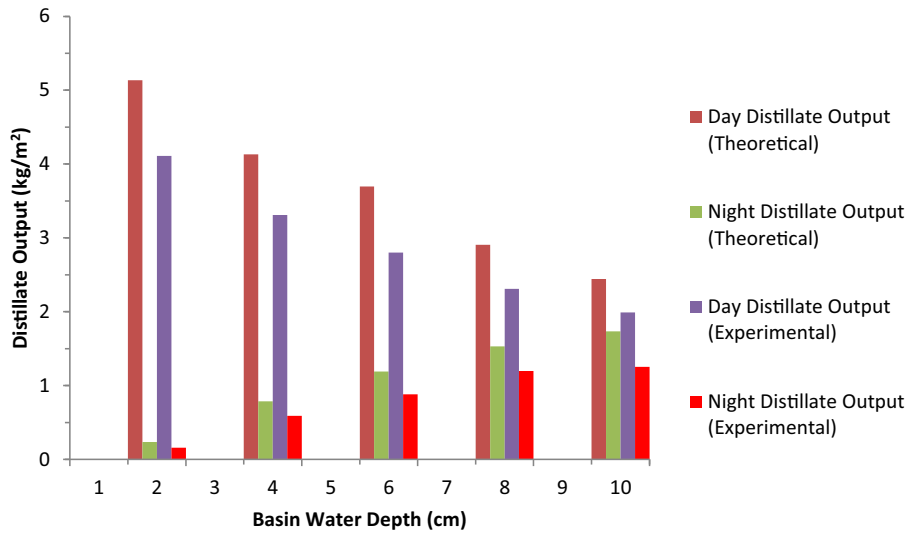


Fig. 15. Theoretical and experimental day and night distillate output of a solar still with different basin water depths.

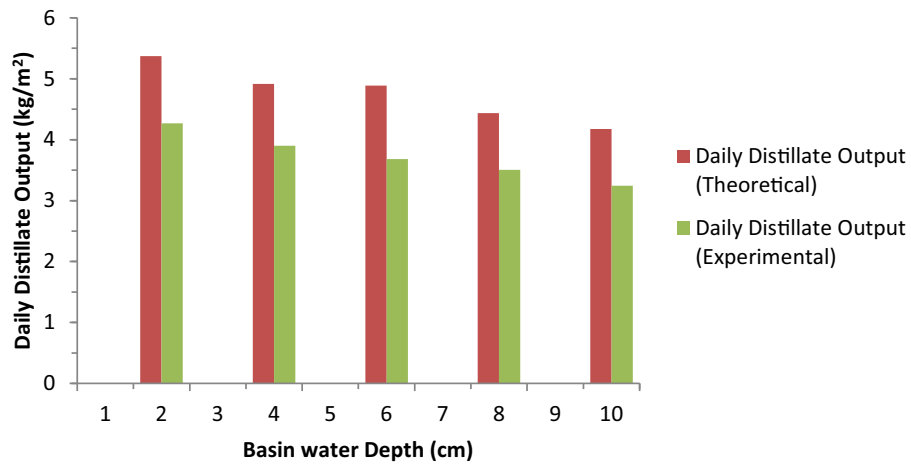


Fig. 16. Theoretical and experimental daily distillate output of solar still with different basin water depths.

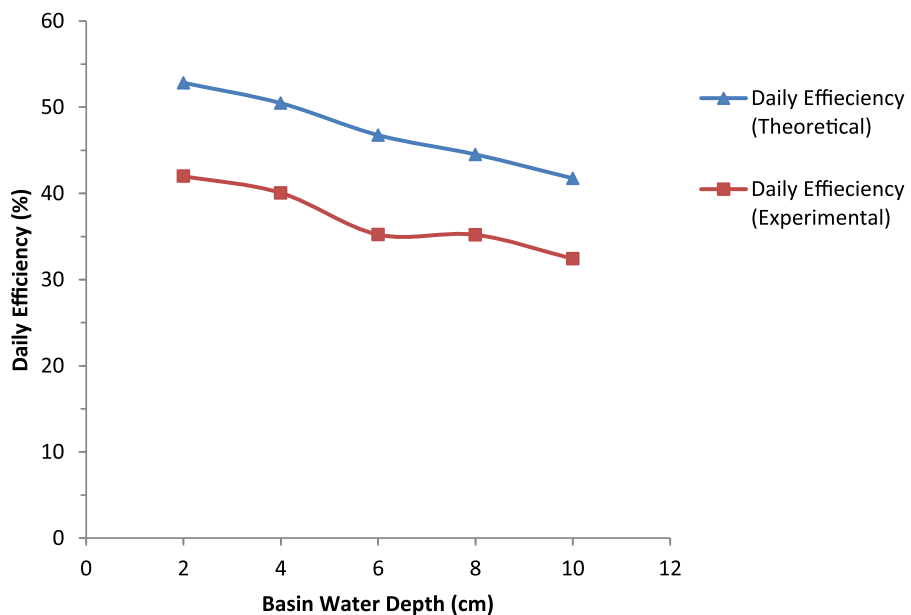


Fig. 17. Theoretical and experimental daily efficiency of solar still with different basin water depths.

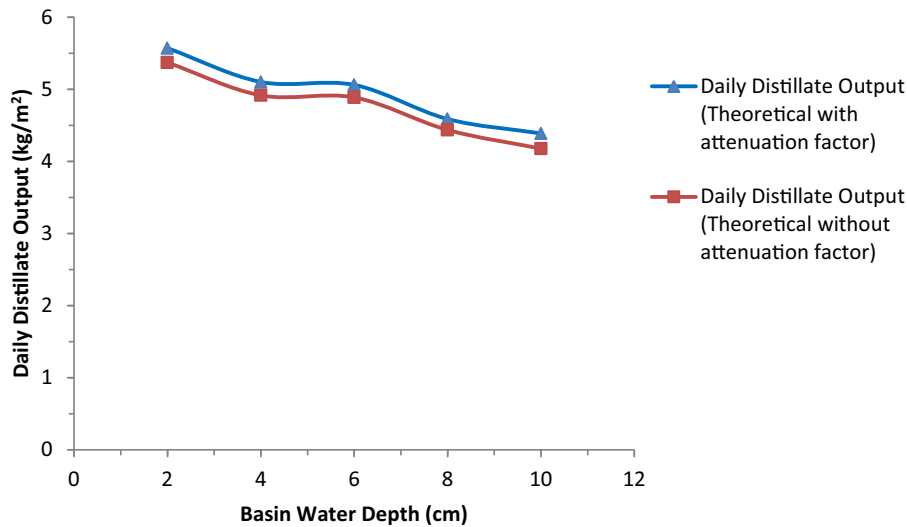


Fig. 18. Comparison of daily distillate output with and without attenuation factor for different basin water depths.

Table 6

Compare the present work with earlier research works.

Sl. No	Author(s)	Type of study	Type of solar still	Productivity (Kg/m ² /day) 2 cm and 10 cm basin water depth	Location/Latitude	Season/month of tests
1.	Yadav and Prasad (1990) [35]	Theoretical	Single basin single slop	5.3 and 4.4	Delhi, India/ 28.37° N	Summer
2.	El-Sebaei et al. (2009) [15]	Theoretical	Single basin single slop	5.5 and 4.5	Jeddah, Saudi Arabia/ 21° 42' N	Summer
3.	Nafey et al. (2002) [36]	Experimental	Single basin single slop	3.1 and 2.1	Suez, Egypt/29.58° N	October and November
4.	Tiwari and Maduhri (1987) [37]	Experimental	Single basin single slop with 35° cover slop	2.9 and 2.2	Delhi, India/ 28.37° N	November
5.	Present research work	Theoretical	Single basin single slop with 24° cover slop	5.37 and 4.17	Rewa, India/24° 33' N	May
		Experimental		4.26 and 3.24		

5.8. Comparison of daily distillate output with and without attenuation factor

Fig. 18 shows the comparison of daily distillate output with and without attenuation factor for different basin water depths. When considering the attenuation factor for different water depths, the distillate output is increased around 4% than without consideration of the attenuation factor for different basin water depths. For 2 cm basin water depth, daily output of solar still with and without attenuation factor is 5.57 kg/m² and 5.37 kg/m² respectively, and for 10 cm water depth, it is 4.38 kg/m² and 4.17 kg/m² respectively.

5.9. Comparison of present research with previous research work

A comparison between productivity values obtained by other researchers and those obtained in the present work is shown in Table 6. Yadav and Prasad [35] obtained theoretically the productivity of single basin solar still as 5.3 Kg/m²/day and 4.4 Kg/m²/day for basin water depths of 2 cm and 10 cm respectively at Delhi, India in the summer season. The theoretical value of productivity of present work for basin water depths of 2 cm and 10 cm respectively for single basin solar still is very close to the above values. Similarly the theoretical values of productivity for 2 cm and 10 cm basin water depths are calculated by El-Sebaei et al [15] is also

very close to the present work. Nafey et al. [36] conducted similar experiments and obtained experimental productivity values as 3.1 Kg/m²/day and 2.1 Kg/m²/day at 2 cm and 10 cm basin water depths respectively.

6. Conclusions

The single slope single basin solar still was fabricated and investigated under the climatic conditions of central part of India at Rewa (Latitude: 24°33' 20.81' N, Longitude: 81°18' 49.1' E). Experimental results for a number of parameters were obtained for the solar still for various basin water depths ranging from 2 cm to 10 cm and these results were compared with the results of theoretical thermal model of solar still. On the basis of present study, the following conclusions can be drawn.

1. The maximum theoretical and experimental values of basin water temperatures are 88 °C and 73 °C at around 13.00 h respectively, for minimum basin water depth (2 cm) while for the maximum basin water depth (10 cm), the values of maximum basin water temperature are 65 °C and 62 °C at around 15.00 h respectively. It shows clearly that the basin water temperature decreases with an increase in the depth of basin water.
2. The maximum theoretical and experimental values of evaporative heat transfer coefficient, obtained by using 2 cm basin

water depth, are $54 \text{ W/m}^2 \text{ }^\circ\text{C}$ and $42 \text{ W/m}^2 \text{ }^\circ\text{C}$, respectively, and minimum values, obtained by using 10 cm basin water depth, are $32 \text{ W/m}^2 \text{ }^\circ\text{C}$ and $26 \text{ W/m}^2 \text{ }^\circ\text{C}$, respectively during 1 p.m. to 3 p.m. It indicates that the evaporative heat transfer coefficient decreases with the increase in basin water depth.

3. It is observed that the values of convective and radiative heat transfer coefficients are much lesser than the value of the evaporative heat transfer coefficient.
4. For 2 cm basin water depth, maximum theoretical and experimental values of distillate output obtained are 830 gm and 742 gm respectively, at 2 p.m. and maximum theoretical and experimental values of distillate output for 10 cm basin water depth are 395 gm and 300 gm respectively, at 3 p.m. It shows that the distillate output decreases with increase in basin water depth in solar still.
5. The theoretical and experimental values of cumulative distillate output for 24 h at lowest basin water depth (2 cm) are $5.37 \text{ kg/m}^2/\text{d}$ and $4.26 \text{ kg/m}^2/\text{d}$ respectively. For highest basin water depth (10 cm), corresponding values are $4.17 \text{ kg/m}^2/\text{d}$ and $3.24 \text{ kg/m}^2/\text{d}$ respectively. It is observed that the cumulative distillate output decreases with increasing basin water depth. Average drinking water need for a human is about 15 per day. Four solar stills of 1 m^2 area can meet this requirement considering the cumulative distillate output for 24 h. These solar stills may be used for potable water in the rural places around Rewa, where the availability of water is insufficient due to hilly region.
6. Nocturnal output is increased with increasing basin water depth. Theoretical and experimental values of the percentage of nocturnal cumulative distillate output for 10 cm basin water depth are obtained as 86% and 75% higher than that for 2 cm basin water depth of solar still.
7. For 2 cm basin water depth, theoretical and experimental daily efficiency is around 52.83% and 41.99%, respectively, and for 10 cm basin water depth, the values are 41.75% and 32.42% respectively. It is clearly observed that the daily efficiency is decreased as the basin water depth increases.
8. When considering the attenuation factor for different basin water depths, the distillate output is increased around 4% than without consideration of the attenuation factor for different basin water depths.
9. The theoretical values of basin water temperature, glass cover temperature, basin temperature, distillate output, and daily efficiency are compared with experimental values. There was good agreement between theoretical and experimental values. The maximum variation is approximately 20%.

Appendix A

Following formula have been used for numerical calculation.

The formulas of partial vapor with the function of temperature are as follows [34]

$$P_w = \text{EXP} \left\{ 25.317 - \frac{5144}{(T_w + 273)} \right\}$$

$$P_g = \text{EXP} \left\{ 25.317 - \frac{5144}{(T_g + 273)} \right\}$$

The effective emittance between the water surface and glass cover is

$$\epsilon_{\text{eff}} = \frac{1}{\left(\frac{1}{\epsilon_w} + \frac{1}{\epsilon_g} - 1 \right)}$$

The latent heat of evaporation of water is calculated by the given expression [38]

$$L_{ev} = (2501.67 - 2.389 \times T_w) \times 10^3 \text{ J/Kg}$$

References

- [1] R.V. Dunkle, Solar water distillation: the roof type still and multiple effect diffusion still, in: International Developments in Heat Transfer, ASME, Proceedings of International Heat Transfer Conference, University of Colorado, 1961, pp. 895–902.
- [2] G.O.G. Lof, J.A. Eibling, J.W. Bloemer, Energy balances in solar distillation, *AIChE J.* 7 (4) (1967) 641–649.
- [3] R.N. Morse, W.R.W. Read, A rational basis for the engineering development of a solar still, *Solar Energy* 12 (1968) 5–17.
- [4] P.I. Cooper, The maximum efficiency of single effect solar still, *Solar Energy* 15 (1973) 205–217.
- [5] P.I. Cooper, Digital simulation of transient solar still processes, *Solar Energy* 12 (1969) 313.
- [6] M.S. Sodha, A. Kumar, G.N. Tiwari, G.N. Pandey, Effects of dye on the performance of a solar still, *Appl. Energy* 7 (1980) 147–162.
- [7] R.S. Adhikari, Ashvini Kumar, Atam Kumar, Estimation of mass-transfer rates in solar stills, *Int J. Energy Res.* 14 (1990) 737–744.
- [8] S. Kumar, G.N. Tiwari, Estimation of convective mass transfer in solar distillation system, *Solar Energy* 57 (1996) 459–464.
- [9] M. Sakthivel, S. Shanmugasundaram, T. Alwarsamy, An experimental study on a regenerative solar still with energy storage medium—jute cloth, *Desalination* 264 (2010) 24–31.
- [10] P.K. Srivastava, S.K. Agrawal, Experimental and theoretical analysis of single sloped basin type solar still consisting of multiple low thermal inertia floating porous absorbers, *Desalination* 311 (2013) 198–205.
- [11] A.A. El-Sebaei, S. Aboul-Enein, E. El-Bialy, Single basin solar still with baffle suspended absorber, *Energy Convers. Manage.* 41 (2000) 661–675.
- [12] Mona M. Naim, Mervat A. Abd El Kawi, Non-conventional solar stills Part I. Non-conventional solar stills with charcoal particles as absorber medium, *Desalination* 153 (1–3) (2003) 55–64.
- [13] A.S. Nafey, M. Abdelkader, A. Abdelmotalip, A.A. Mabrouk, Solar still productivity enhancement, *J. Energy Convers. Manage.* 42 (2001) 1401–1408.
- [14] Salah Abdallah, Mazen M. Abu-Khade, Omar Badran, Effect of various absorbing materials on the thermal performance of solar stills, *Desalination* 242 (2009) 128–137.
- [15] A.A. El-Sebaei, A.A. Al-Ghamdi, F.S. Al-Hazmi, Adel S. Faidah, Thermal performance of a single basin solar still with PCM as a storage medium, *Appl. Energy* 86 (2009) 1187–1195.
- [16] G.N. Tiwari, J.M. Thomas, Emran Khan, Optimization of glass cover inclination for maximum yield in a solar still, *Heat Recovery Syst. CHP* 14 (1994) 447–455.
- [17] V. Velmurugan, M. Gopalakrishnan, R. Raghu, K. Srithar, Single basin solar still with fin for enhancing productivity, *J. Energy Convers. Manage.* 49 (2008) 2602–2608.
- [18] Pankaj K. Srivastava, S.K. Agrawal, Winter and summer performance of single sloped basin type solar still integrated with extended porous fins, *Desalination* 319 (2013) 73–78.
- [19] Z.M. Omara, Mofred H. Hamed, A.E. Kabeel, Performance of finned and corrugated absorber solar stills under Egyptian conditions, *Desalination* 277 (2011) 281–287.
- [20] Hiroshi Tanaka, Yasuhito Nakatake, Theoretical analysis of a basin type solar still with internal and external reflector, *Desalination* 197 (2006) 205–216.
- [21] Narjes Setoodeh, Rahbar Rahimi, Abolhasan Ameri, Modeling and determination of heat transfer coefficient in a basin solar still using CFD, *Desalination* 268 (2011) 103–110.
- [22] G.N. Tiwari, in: *Solar Energy*, Narosa Publishing House, New Delhi, India, 2002, pp. 279–309.
- [23] S.K. Shukla, V.P.S. Sorayan, Thermal modeling of solar stills an experimental validation, *Renewable Energy* 30 (2005) 683–699.
- [24] M.A.S. Malik, V.A. Tran, Simple mathematical model for predicting the nocturnal output of a solar still, *Solar Energy* 14 (4) (1973) 371–385.
- [25] S. Kumar, G.N. Tiwari, H.N. Singh, Annual performance of active solar distillation system, *Desalination* 127 (1) (2000) 79–88.
- [26] J.M. Pearce, D. Denkenberger, Numerical simulation of the direct application of compound parabolic concentrators to a single effect basin solar still, in: Proceedings of the 2006 International Conference of Solar Cooking and Food Processing, 2006, p. 118.
- [27] J.H. Watmuff, W.W.S. Charters, D. Proctor, Solar and wind induced external coefficient for solar collectors, Technical Note, *COMPLES* 2 (1977) 56.
- [28] J.A. Duffie, W.A. Beckman, in: *Solar Engineering of Thermal Processes*, John Wiley & Sons, New West Editions, New York, 1980, pp. 173–176.
- [29] A.K. Tiwari, G.N. Tiwari, Thermal modeling based on solar fraction and experimental study of annual and seasonal performance of a single slope passive solar still: the effect of water depths, *Desalination* 207 (2007) 184–204.
- [30] V. Velmurugan, C.K. Deenadayalan, H. Vinod, K. Srithar, Desalination of effluent using fin type solar still, *Energy* 33 (2008) 1719–1727.
- [31] J.P. Holman, *Experimental Method for Engineering*, sixth ed., McGraw-Hill, Singapore, 1994.

- [32] H.A. Zoori, F.F. Tabrizi, F. Sarhaddi, F. Heshmatnezhad, Comparison between energy and exergy efficiencies in a weir type cascade solar still, *Desalination* 325 (2013) 113–121.
- [33] E. Sartori, Solar still versus evaporator: a comparative study between thermal behaviors, *Solar Energy* 56 (No.2) (1996) 199–206.
- [34] M.K. Gaur, G.N. Tiwari, Optimization of number of collectors for integrated PV/T hybrid active solar still, *Appl. Energy* 87 (2010) 1763–1772.
- [35] Y.P. Yadav, Y.N. Prasad, Parametric investigation on a basin type solar still, *Energy Convers. Manage.* 31 (1) (1991) 7–16.
- [36] A.S. Nafey, M. Abdelkader, A. Abdelmotalip, A.A. Mabrouk, Enhancement of solar still productivity using floating perforated black plate, *Energy Convers. Manage.* 43 (2002) 937–946.
- [37] G.N. Tiwari Madhuri, Effect of water depth on daily yield of the still, *Desalination* 61 (1987) 67–75.
- [38] H.E.S. Fath, H.M. Hosny, Thermal performance of a single sloped basin still with an inherent built-in additional condenser, *Desalination* 142 (2002) 19–27.